NASA TECHNICAL NOTE

NASA TN D-4196

c. 1

NASA TN D-4196

PRESSURES AND FORCES ON FLARE-STABILIZED BODIES IN AIR AND IN A MIXTURE OF 85-PERCENT CO_2 AND 15-PERCENT AIR

by Gene P. Menees

Ames Research Center
Moffett Field, Calif.

NATIONAL AERONAUTICS AND SPACE ADMINISTRATION • WASHINGTON, D. C. • OCTOBER 1967

NASA TN D-4196

PRESSURES AND FORCES ON FLARE-STABILIZED BODIES IN AIR AND IN A MIXTURE OF 85-PERCENT CO_2 AND 15-PERCENT AIR

By Gene P. Menees

Ames Research Center
Moffett Field, Calif.

NATIONAL AERONAUTICS AND SPACE ADMINISTRATION

For sale by the Clearinghouse for Federal Scientific and Technical Information
Springfield, Virginia 22151 – CFSTI price $3.00

PRESSURES AND FORCES ON FLARE-STABILIZED BODIES IN AIR AND IN A MIXTURE OF 85-PERCENT CO_2 AND 15-PERCENT AIR

By Gene P. Menees

Ames Research Center

SUMMARY

The effect of gas composition on the aerodynamic characteristics of flare-stabilized bodies was studied experimentally. Pressure distributions were obtained on flare-stabilized cylinders with three different nose shapes. The tests were made at Mach numbers of 5.2 and 7.4 in air and 5.7 in a mixture of 85-percent CO_2 and 15-percent air. The nose shapes were a 22-1/2° half-angle cone, a hemisphere, and a near ellipsoid. The flare was a frustum with a cone angle of 16.5°. So that the experimental results could be compared directly with inviscid theories, most of the pressure data were measured with a gap between the flare and the body to bleed off the boundary layer at the flare-cylinder junction. This technique eliminated large regions of flare-induced flow separation on the cylindrical bodies.

The results of the present study showed that the aerodynamic coefficients were essentially the same in air and in the CO_2-air mixture for all test models, both with and without flow separation. Predictions made with various inviscid theories agreed well with the experimental results for the conical- and hemispherical-nosed models but were not in good agreement with the results for the near ellipsoidal-nosed model.

INTRODUCTION

Previous experimental and analytical studies (refs. 1 and 2) have shown that the aerodynamic characteristics of entry bodies might be sensitive to the nitrogen-carbon dioxide atmospheres thought to exist on Mars and Venus. In particular, reference 1 reports that the static stability of a blunt-nosed, flare-stabilized body is significantly less in carbon dioxide than in air and attributes this result to the high degree of caloric imperfection of carbon dioxide. Since such effects could have an important influence on the trajectory and motion of bodies flying in planetary atmospheres containing large amounts of carbon dioxide, additional experimental studies were made to define better the various gasdynamic factors governing the flow of carbon dioxide over flare-stabilized bodies.

Surface pressures were measured on three flare-stabilized cylindrical bodies that differed only in nose shape. Data were obtained in the Ames

3.5-Foot Hypersonic Wind Tunnel at Mach numbers of 5.2 and 7.4 in air and 5.7 in a mixture of 85-percent CO_2 and 15-percent air. To minimize flare-induced flow separation and effects of shock-wave boundary-layer interaction, most of the tests were made with models having a small gap between the body and flare for boundary-layer removal to allow a direct comparison of the data and inviscid theories.

SYMBOLS

A	reference area, $\frac{\pi d^2}{4}$
C_A	axial force coefficient (excluding viscous and base contributions), $\frac{\text{axial force}}{q_\infty A}$
C_N	normal-force coefficient, $\frac{\text{normal force}}{q_\infty A}$
$\left(C_{N_\alpha}\right)_{\alpha=0}$	derivative of C_N with respect to angle of attack evaluated at zero angle of attack, per rad
C_p	model surface pressure coefficient, $\frac{p - p_\infty}{q_\infty}$
d	diameter of cylindrical body segment
M_∞	free-stream Mach number
p	surface pressure
p_∞	free-stream pressure
q_∞	free-stream dynamic pressure
x_{cp}	distance from body nose to center of pressure
x,r	rectangular coordinates with origin at body nose
α	angle of attack, deg
γ	ratio of specific heats

EXPERIMENT

Models and Instrumentation

The test models, shown in figure 1, had a cylindrical center section, three interchangeable noses, and two interchangeable flares. The nose shapes were a 22-1/2° half-angle cone, a hemisphere, and a near ellipsoid. The flares were frustums of a 16.5° cone. One flare was integral with the body while the other was designed to allow removal of the boundary layer at the cylinder-flare junction in order to suppress flare-induced flow separation on the cylindrical portion of the body. The technique used to remove the boundary layer was to make the flare hollow and to provide a gap between the flare and body cylinder through which the boundary layer could flow. The gap was approximately 5 percent of the diameter of the body cylinder. The models had pressure orifices distributed in two rows, 180° apart.

Facility and Test Procedure

The experimental investigation was conducted in the Ames 3.5-Foot Hypersonic Wind Tunnel at Mach numbers of 5.2 and 7.4 in air and 5.7 in an 85-percent CO_2, 15-percent air mixture. The nozzle contoured for $M = 7.4$ in air was used for the tests in the CO_2-air mixture. This resulted in a Mach number of 5.7 for the mixture. Calibrations of this nozzle with the CO_2-air mixture showed that the quality of the flow was very good and equal to the flow quality when air was used as the test medium. The stagnation pressures for the air tests were 13.6 and 102.0 atm (200 and 1500 psia) for Mach numbers 5.2 and 7.4, respectively, and 68.1 atm (1000 psia) for the tests in the CO_2-air mixture. All tests were made at a constant stagnation temperature of 1055° K. The corresponding Reynolds numbers per foot were approximately 0.9×10^6 and 3.6×10^6, respectively, at Mach numbers 5.2 and 7.4 in air and 2.0×10^6 at the Mach number of 5.7 in the CO_2-air mixture. Data were taken at angles of attack of approximately 0°, 5°, and 10°. An average test took approximately 1 minute. A more general description of the test facility and its instrumentation is given in reference 3. For the present tests, the models were inserted into the test section only after steady flow was established.

RESULTS AND DISCUSSION

The results of the investigation are presented in figures 2 through 7. Measured surface pressures in coefficient form and predictions made with inviscid theories (see ref. 4) are presented in figures 2, 3, and 4 for the conical-, hemispherical-, and near ellipsoidal-nosed models, respectively. The theories consist of the method of characteristics in combination with a conical flow solution for the conical-nosed model and with a blunt-body solution for the two blunt-nosed models. The inviscid theories are compared with the data for the models with the gap for boundary-layer removal. Some pressure distributions are also shown for the models at zero angle of attack without the gap in order to illustrate the effectiveness of the gap in eliminating flow separation. Force coefficients and centers of pressure obtained by integrating the longitudinal pressure distributions, with assumed cosine variations in circumferential pressure distribution, are presented in figures 5 to 7. Both the variations with angle of attack for Mach number 5.2 in air and 5.7 in the CO_2-air mixture and the variations with Mach number for zero angle of attack are shown. Air results for the conical- and hemispherical-nosed models have been reported previously in reference 4. It was noted in reference 4 that for the hemispherical-nosed model the experimental data deviate from the assumption of a cosine variation for the circumferential pressure distribution. However, the errors resulting from this assumption were canceled when normal force and pitching moment were computed. This was verified by comparing the computed results with results of force tests made for each of the test models with the flare and no gap. In all cases, the measured force coefficients agreed within 10 percent of the values obtained by integrating the model surface pressures as previously described.

Pressure Distributions

Conical-nosed model.- Experimental surface pressure coefficients for the conical-nosed model are compared in figure 2 with values predicted by theory for equilibrium flow. The predicted results for nonzero angle of attack were obtained by using a tangent cone approximation (i.e., increasing and decreasing the body slopes by the angle of attack). The agreement between the measured results and those predicted by equilibrium theory is generally very good. The only notable difference occurs on the flare at zero angle of attack for Mach number 5.7 in the CO_2-air mixture (see fig. 2(c)), where the experimental results are about 25 percent higher than predicted by the equilibrium theory. An attempt was made to determine if this difference could be a result of vibrational nonequilibrium in the flow over the model. Various nonequilibrium flow conditions were assumed to exist on the model and the resulting surface pressures were calculated. The conditions considered were: (1) perfect gas, (2) equilibrium free stream with frozen flow over the model, and (3) flow frozen at first Mach line from shoulder. The predicted results for these conditions are also shown in figure 2(c). It is seen that condition (2) gives the best overall agreement with the experimental pressures at zero angle of attack but still predicts pressures smaller than those measured on the flare. Additional calculations based on model geometry and relaxation time of the CO_2-air mixture indicate that condition (2) is possible for the current tests. From the angle-of-attack results, however, it is apparent that there is little difference between the equilibrium and various assumed nonequilibrium conditions.

Hemispherical-nosed model.- The experimental results for the hemispherical-nosed model are compared in figure 3 with values predicted by theory. The pressures on the forward portion of the hemisphere are not shown in the figure; however, the agreement between theory and experiment was very good in this region for all test conditions. A detailed discussion of the results of the air tests for this model along with an analysis of the perturbation method used to obtain angle-of-attack results can be found in reference 4. For the tests in the CO_2-air mixture (fig. 3(c)), good agreement is obtained with the equilibrium theory except on the flare of the model. The disagreement at angle of attack is not surprising because of the limitations of the perturbation method (see ref. 4). However, the fact that the flare pressures are slightly higher than the equilibrium theory at $\alpha = 0^{\circ}$ possibly indicates that in this region the flow may not be in equilibrium. Another possible flow condition, that of a perfect gas, is also shown on figure 3(c) for comparative purposes. It can be seen that better agreement is obtained with the measured flare pressures than was given by the equilibrium solution, but poorer agreement results on the forward part of the body.

Ellipsoidal-nosed model.- The experimental results for the near ellipsoidal-nosed model are presented in figure 4. No solutions could be obtained from the inviscid theory for $M = 5.2$ and only solutions for zero angle of attack could be obtained for the other test conditions. The experimental pressures at $\alpha = 0^{\circ}$ agree well with the equilibrium solutions except on the flare of the model for the tests in the CO_2-air mixture (see fig. 4(c)). Here, as was the case for the hemispherical-nosed model, the experimental pressures are slightly higher than predicted by equilibrium theory. Also shown on figure 4(c) is a perfect-gas solution. The experimental data are about halfway between the equilibrium and perfect-gas solutions on the flare of the model, but are in better agreement with the equilibrium solution on the forward portion of the cylinder.

Forces and Center of Pressure

Aerodynamic force coefficients, obtained from integration of the experimental longitudinal pressure distributions with assumed cosine circumferential variation, are presented in figures 5, 6, and 7 for the conical-, hemispherical-, and near ellipsoidal-nosed models, respectively. The results of various theories are also shown. Both the variations with angle of attack and with Mach number are given. In the calculations of the slopes of the normal-force coefficients and the centers of pressure at $\alpha = 0^{\circ}$ variations with angle of attack were assumed to be linear from 0° to 5°.

Conical-nosed model.- The results for the conical-nosed model, presented in figure 5, generally agree closely with the inviscid theory. The theory also predicts little difference between results obtained in air and in the CO_2-air mixture for various assumed flow conditions.

Hemispherical-nosed model.- The experimental results for the hemispherical-nosed model (fig. 6) are in excellent agreement with those predicted by theory up to $\alpha = 5^{\circ}$, and the theory predicts no difference between equilibrium air and the equilibrium or perfect gas for the CO_2-air mixture. Results predicted by the method of reference 5 are also shown in figure 6. This method predicts normal-force coefficients that are too large for both air and the CO_2-air mixture but correctly predicts axial force and center-of-pressure location. Also, the predicted lift-curve slope for equilibrium air is about 20 percent higher than that for the equilibrium CO_2-air mixture, but about the same as that for the perfect-gas condition for the mixture. Therefore, depending on the degree of nonequilibrium of the CO_2-air mixture, the method of reference 5 predicts that the static stability of this model could be lower or about the same as the stability in equilibrium air. One would expect, however, that the predictions of the more exact blunt body and method of characteristics theory, which show no effect of gas composition, would be more indicative of the actual situation than the predictions from the method of reference 5.

Ellipsoidal-nosed model.- The experimental force coefficients for the near ellipsoidal-nosed model are presented in figure 7 and, as was the case for the other test models, show no difference between the tests in air and in the CO_2-air mixture. The experimental results are compared with values predicted by the methods of references 2 and 5 since these were the only analytical methods available for this model. Both methods predict lift-curve slopes that are too large and show the lift in equilibrium air to be greater than the lift in the equilibrium CO_2-air mixture. However, when the method of reference 5 was also used for a perfect-gas CO_2-air mixture, the lift was greater than the lift for equilibrium air. Both methods agree well with the axial force; however, the method of reference 5 gives a better prediction of center-of-pressure location. A comparison of the predicted lift-curve slopes and centers of pressure in figure 7 shows that the methods of both references 2 and 5 will predict a lower static stability in the equilibrium CO_2-air mixture than in equilibrium air. Also, the method of reference 5 predicts that the model would be less stable in equilibrium air if the CO_2-air mixture approaches the state of a perfect gas. Therefore, depending on the state of the CO_2-air mixture, there is a considerable uncertainty in static stability. It is unfortunate that calculations with the blunt body and method of characteristics theory could not be made to better determine the effect of gas composition for this model.

CONCLUDING REMARKS

The results of the present tests show that the aerodynamic coefficients measured in air and in the 85-percent CO_2 and 15-percent air mixture were essentially the same for all test models both with and without flow separation. Predictions made with various inviscid theories agreed well with the experimental results for the conical- and hemispherical-nosed models but were not in good agreement with the results for the near ellipsoidal-nosed model.

The results of the present tests showing practically no effect of gas composition on static stability differ from the free-flight test results of reference 1 which indicate that static stability may be significantly less in CO_2 than in air. This difference cannot be resolved from the information currently available. However, a possible explanation is that the CO_2 in the present tests was out of equilibrium over the afterportion of the models because of vibrational relaxation. In addition, some flare-induced flow separation was detectable on the models in the tests of reference 1. This might possibly have had a different influence on the stability of the models in CO_2 and air than the separation which occurred on the models with the conventional flare in the present tests. It is of interest to note that other investigators have reported seemingly conflicting effects of gas composition on the static stability of the shape having the near ellipsoidal nose. Results summarized in reference 6 show significant differences in static stability between tests made in air and helium but no difference between tests made in nitrogen and helium. This is unexpected since air and nitrogen have similar thermodynamic properties.

Ames Research Center
National Aeronautics and Space Administration
Moffett Field, Calif., 94035, June 19, 1967
124-07-02-13-00-21

REFERENCES

1. Menees, Gene P.; and Smith, Willard G.: A Study of the Stability and Drag of Several Aerodynamic Shapes in Air, Carbon Dioxide, and Argon at Mach Numbers From 3 to 8. NASA TM X-950, 1964.

2. Jorgensen, Leland H.; and Graham, Lawrence A.: Predicted and Measured Aerodynamic Characteristics for Two Types of Atmosphere-Entry Vehicles. NASA TM X-1103, 1965.

3. Polek, Thomas E.; Holdaway, George H.; and Kemp, Joseph H., Jr.: Flow Field and Surface Pressures on a Blunt Half-Cone Entry Configuration at Mach Numbers of 7.4 and 10.4. NASA TM X-1014, 1964.

4. Rakich, John V.; and Menees, Gene P.: A Theoretical and Experimental Study of Hypersonic Flow Over Flared Bodies at Incidence. NASA TN D-3218, 1966.

5. Seiff, Alvin: Atmosphere Entry Problems of Manned Interplanetary Flight. Proc. AIAA and NASA Conf. on Engineering Problems of Manned Interplanetary Exploration, Palo Alto, Calif., Sept. 30-Oct. 1, 1963, pp. 19-33.

6. Arrington, J. P.; and Henderson, A., Jr.: Effects of Reynolds Number on the Stability of a Blunt-Nosed Flared Cylinder From Mach 17.6 to 22.2 in Helium. NASA TM X-1166, 1965.

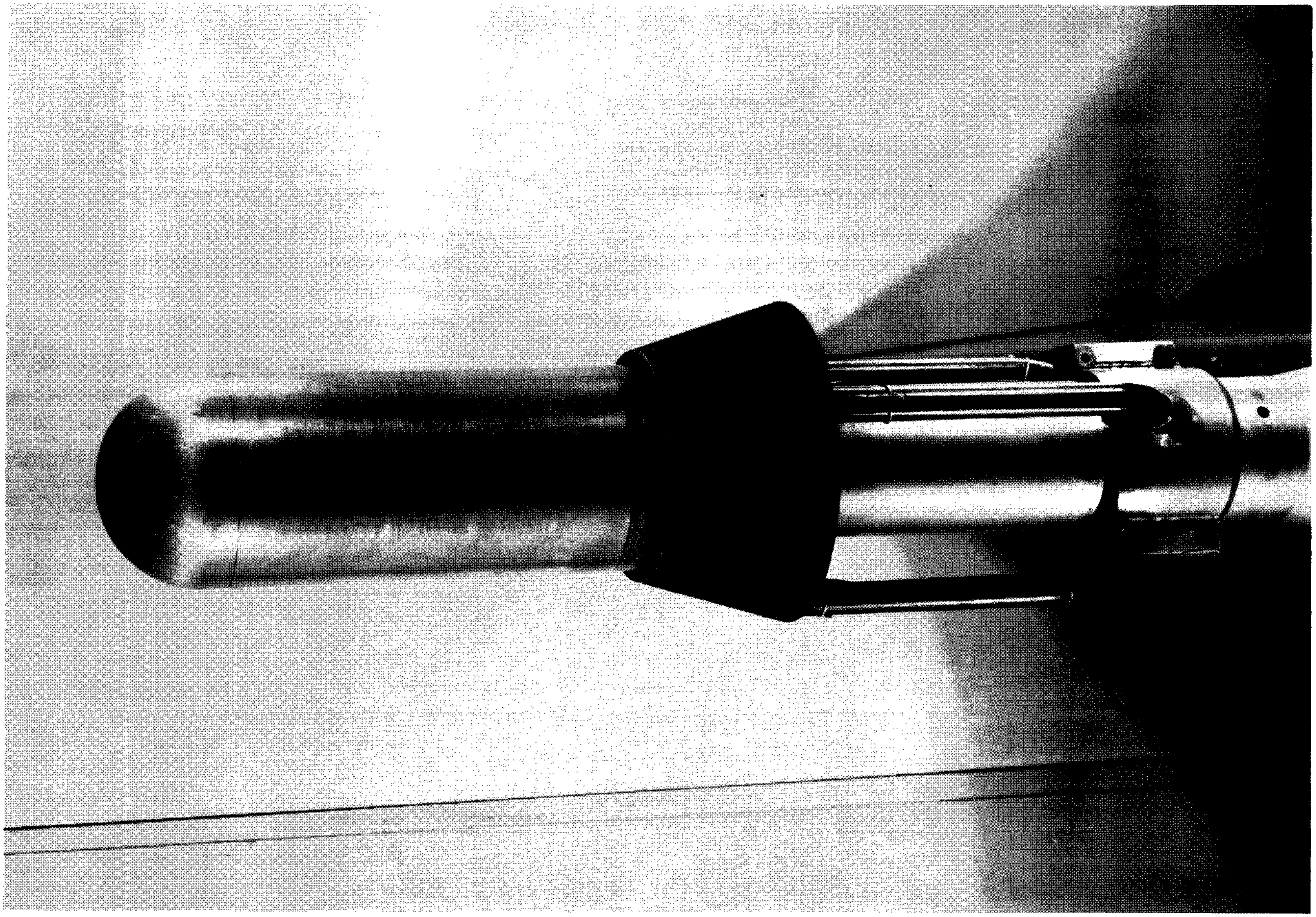

A-37409

(a) Hemispherical-nosed model with gap mounted in 3.5-Foot Hypersonic Wind Tunnel.

Figure 1.- Wind-tunnel models.

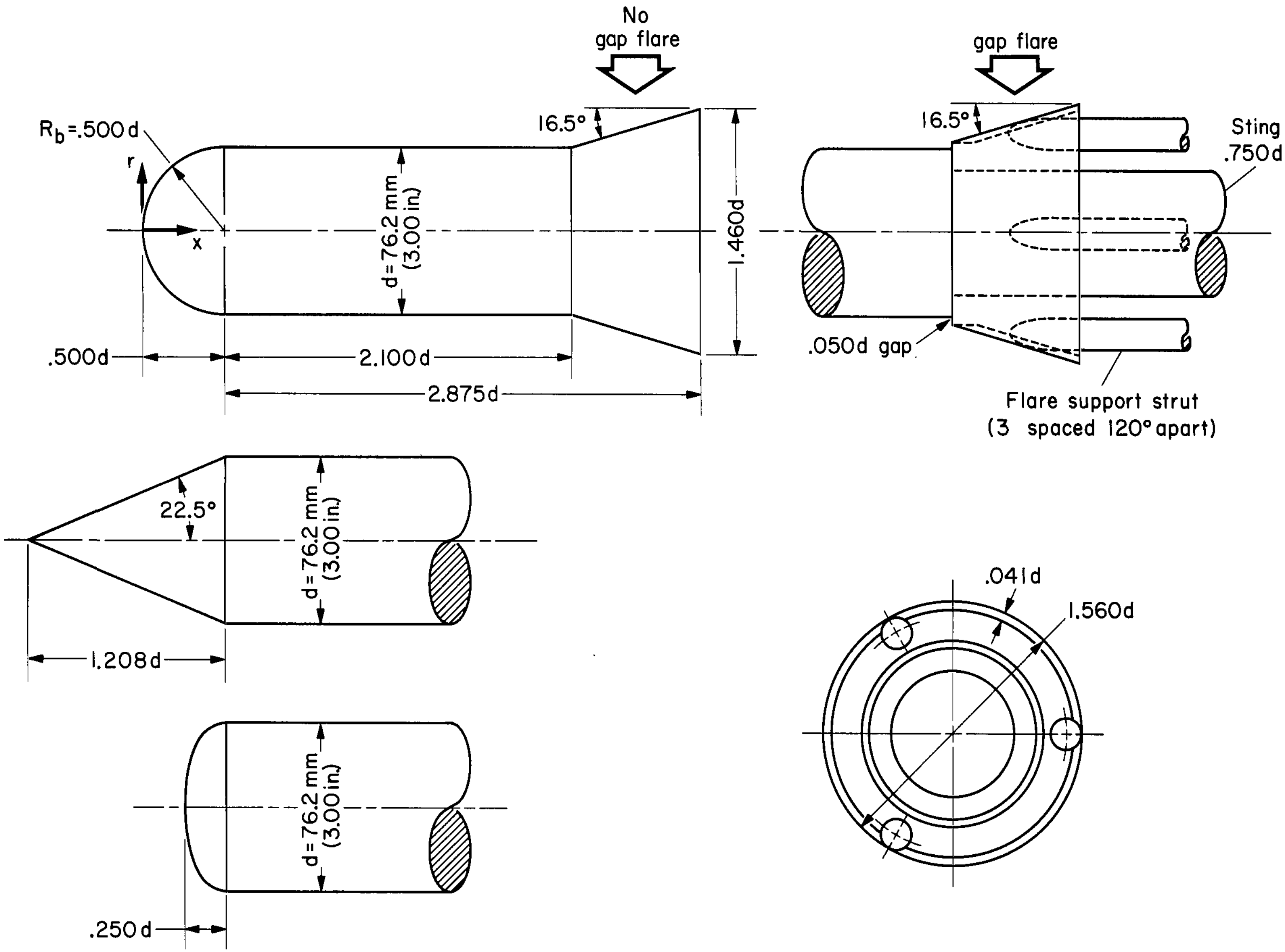

(b) Dimensions.

Figure 1.- Concluded.

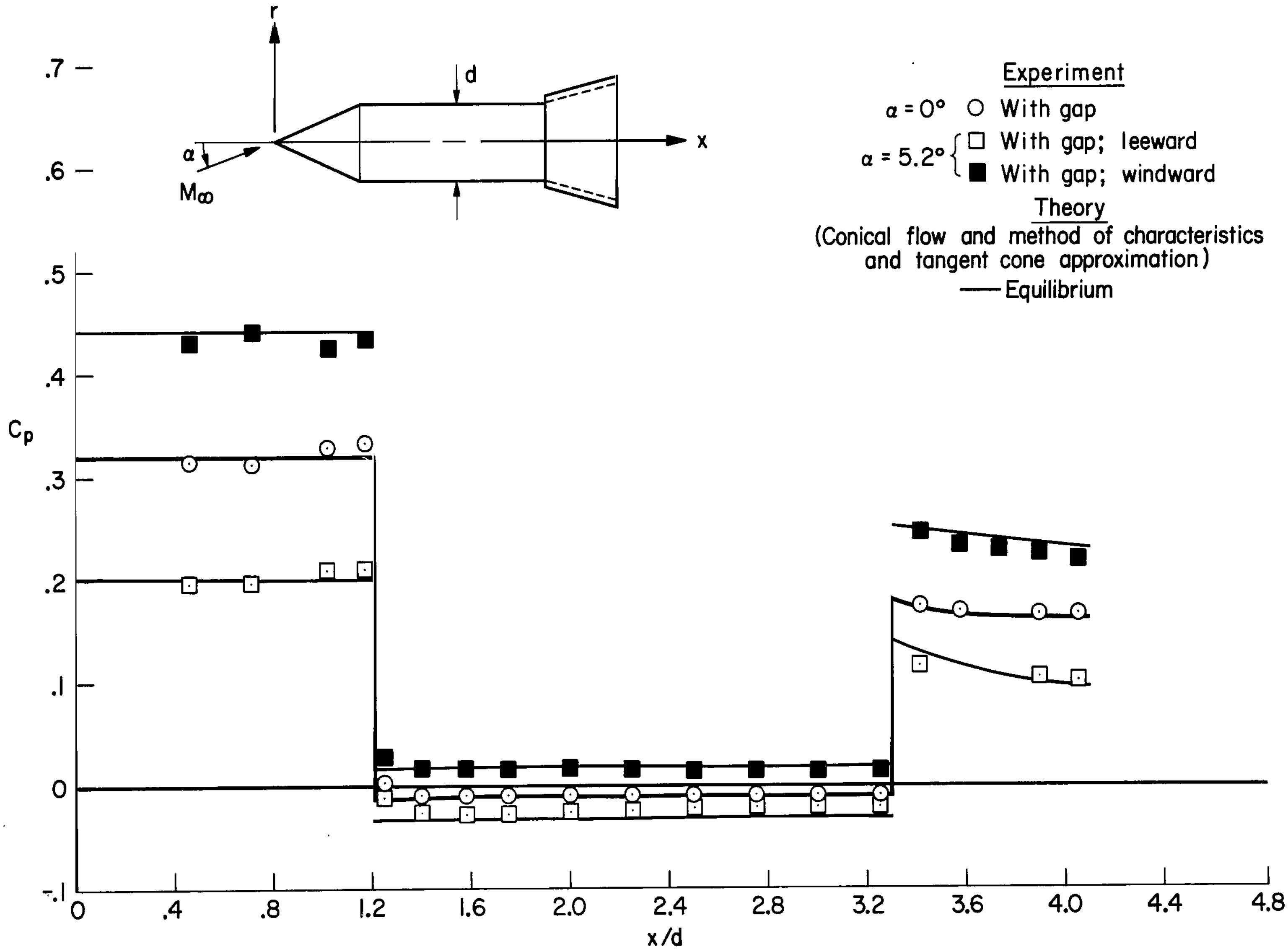

(a) Air, M_∞ = 5.2

Figure 2.- Measured and predicted surface-pressure distributions for the conical-nosed model.

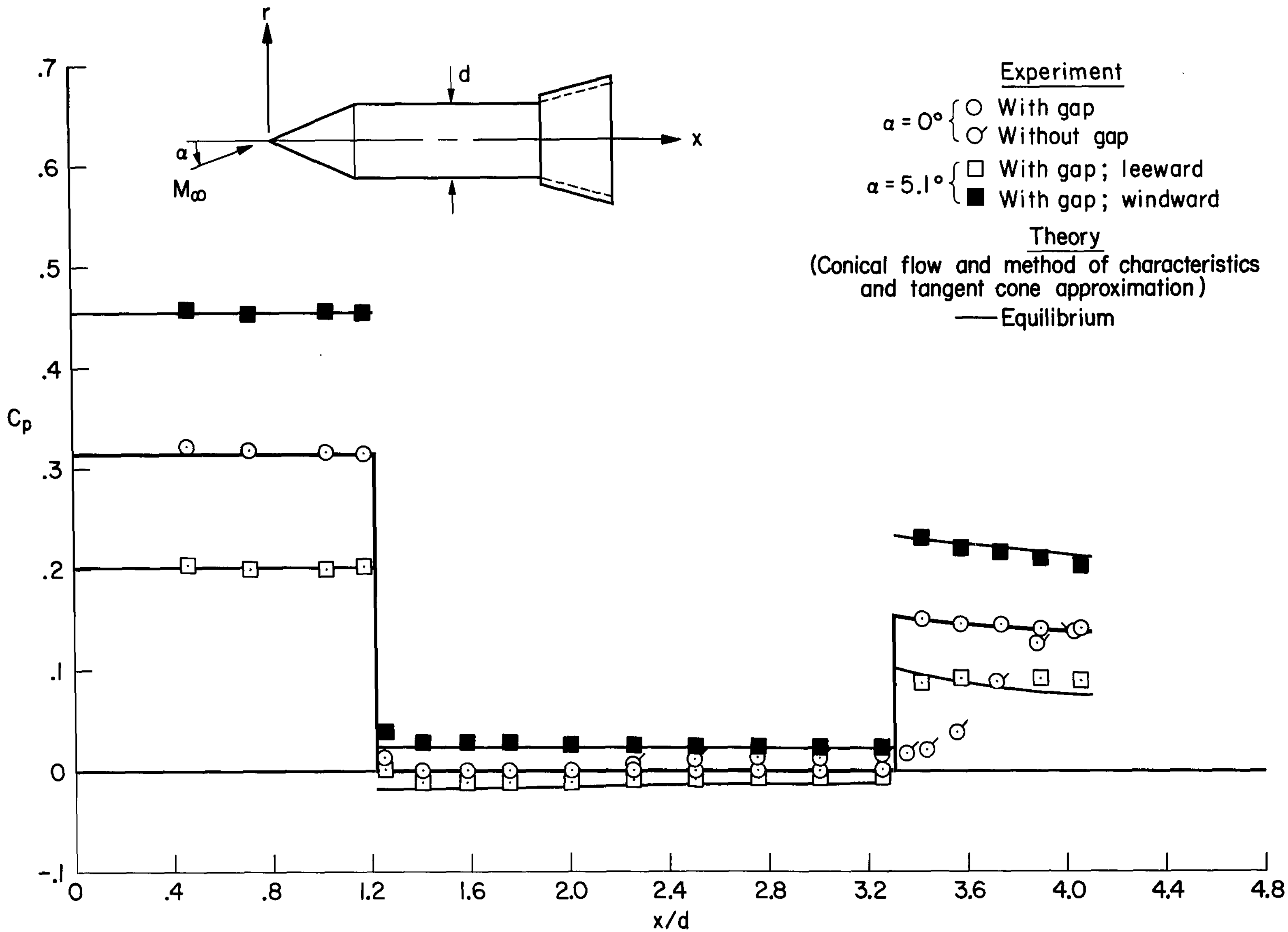

(b) Air, $M_\infty = 7.4$

Figure 2.- Continued.

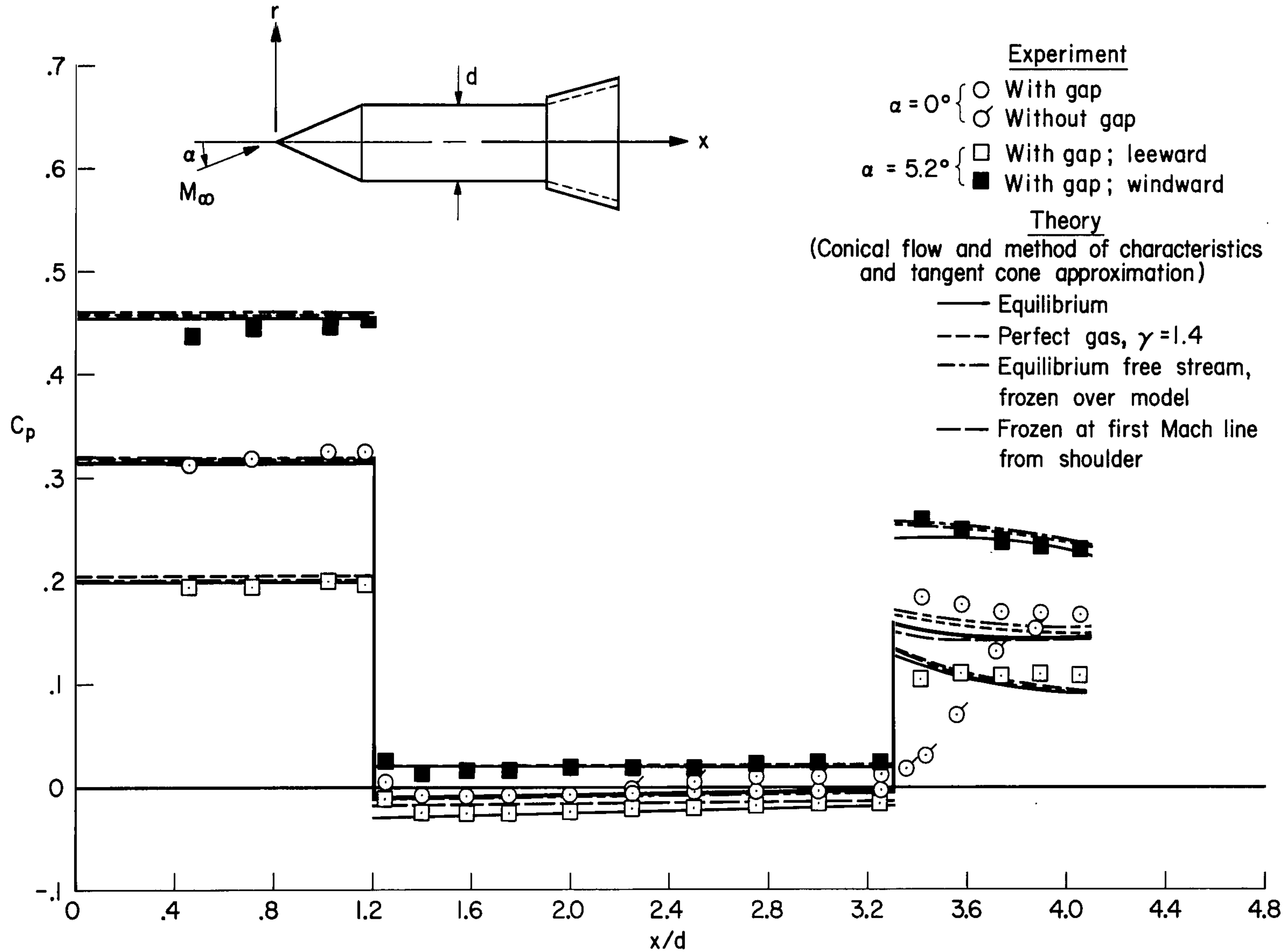

(c) 85-percent CO_2, 15-percent air; $M_\infty = 5.7$

Figure 2.- Concluded.

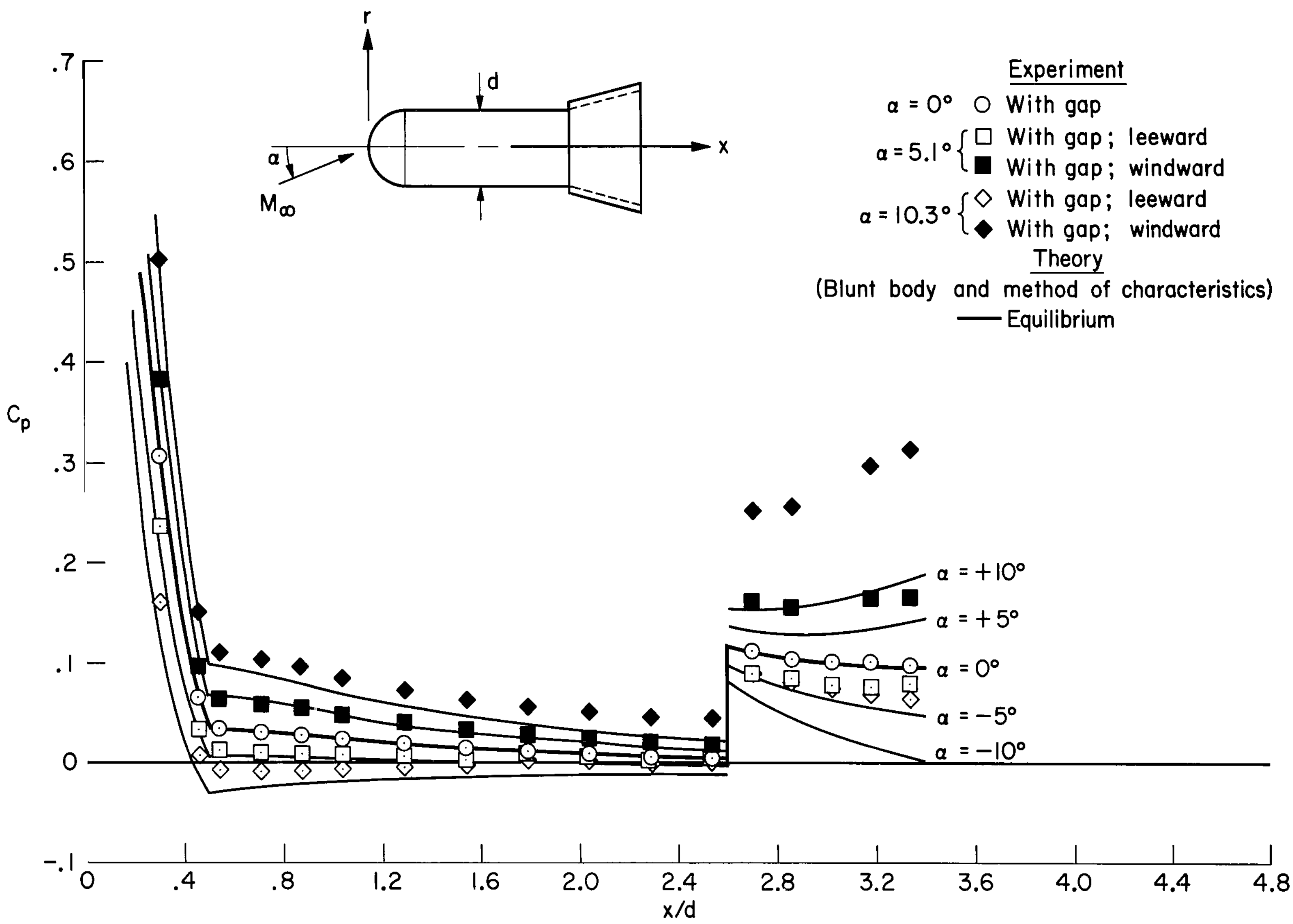

(a) Air, $M_\infty = 5.2$

Figure 3.- Measured and predicted surface-pressure distributions for the hemispherical-nosed model.

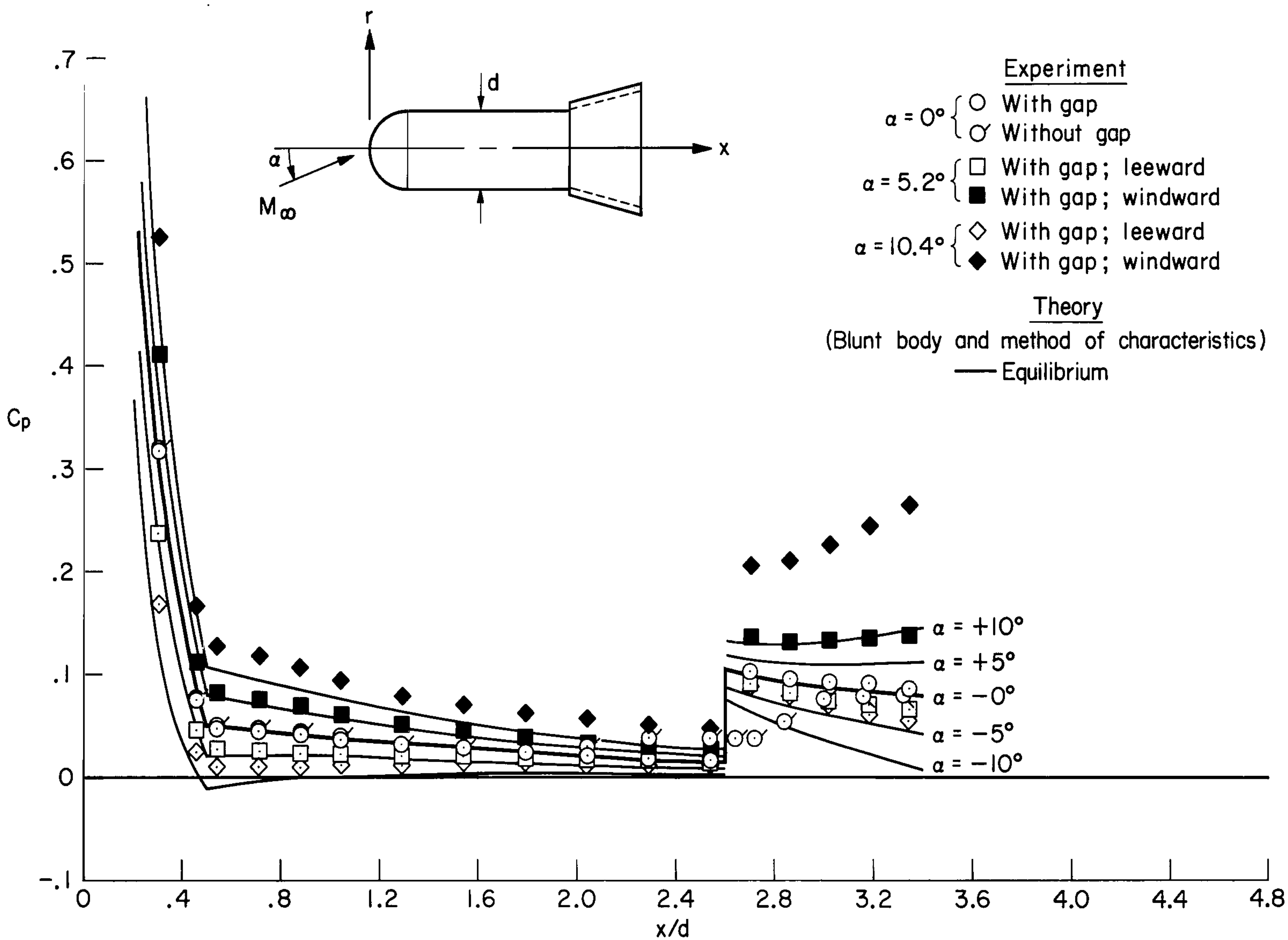

(b) Air, M_∞ = 7.4

Figure 3.- Continued.

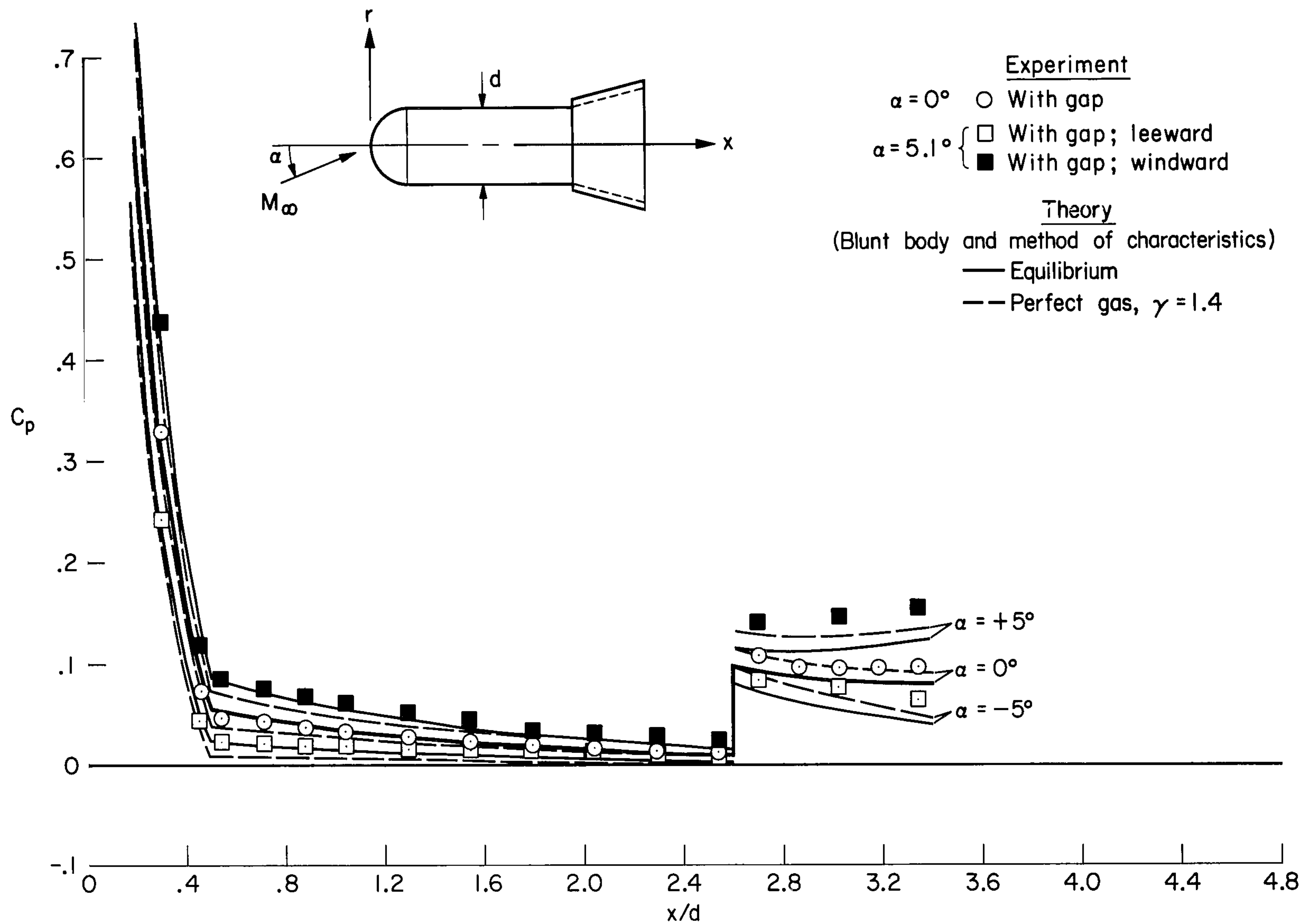

(c) 85-percent CO_2, 15-percent air; $M_\infty = 5.7$

Figure 3.- Concluded.

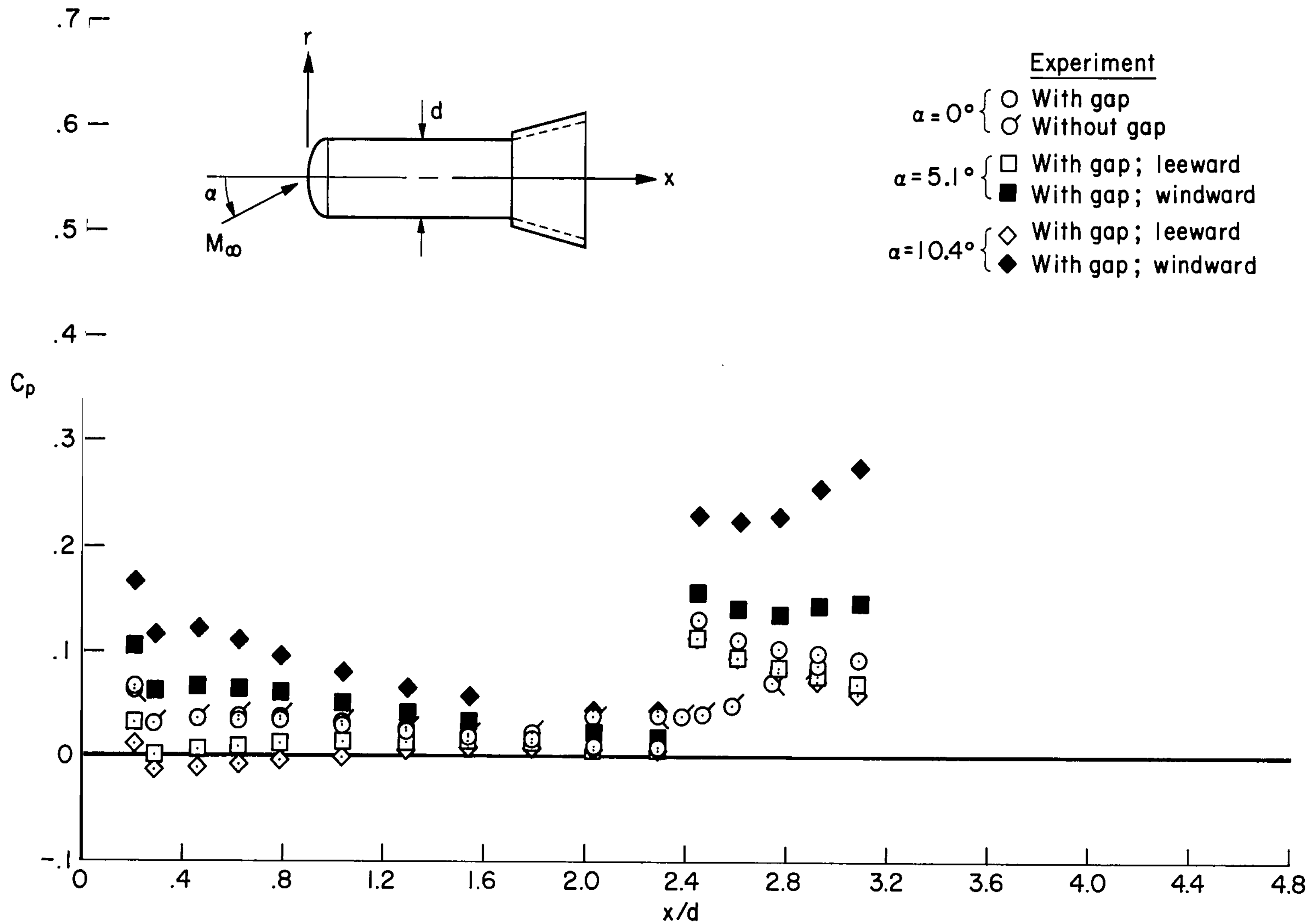

(a) Air, M_∞ = 5.2

Figure 4.- Measured and predicted surface-pressure distributions for the near ellipsoidal-nosed model.

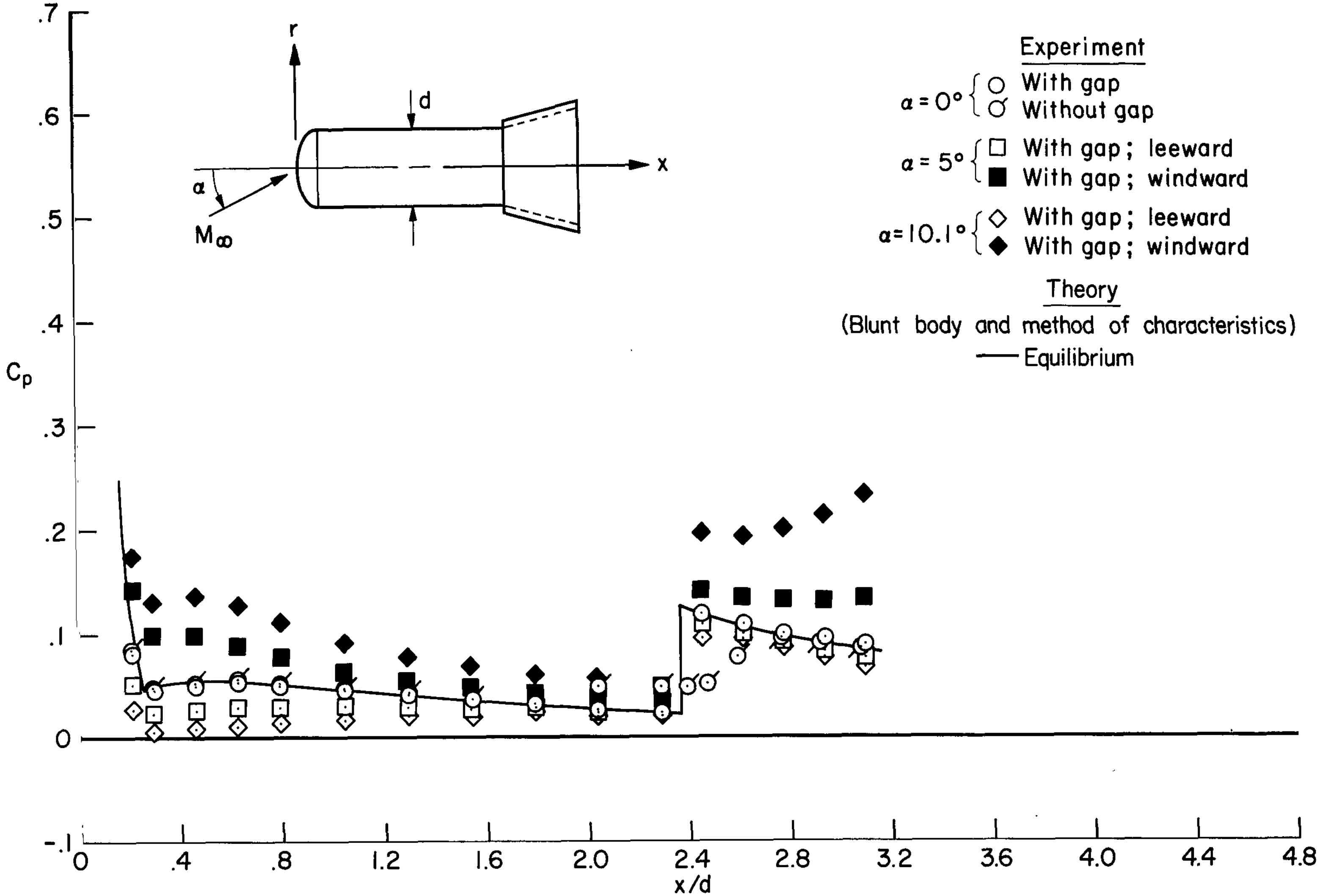

(b) Air, $M_\infty = 7.4$

Figure 4.- Continued.

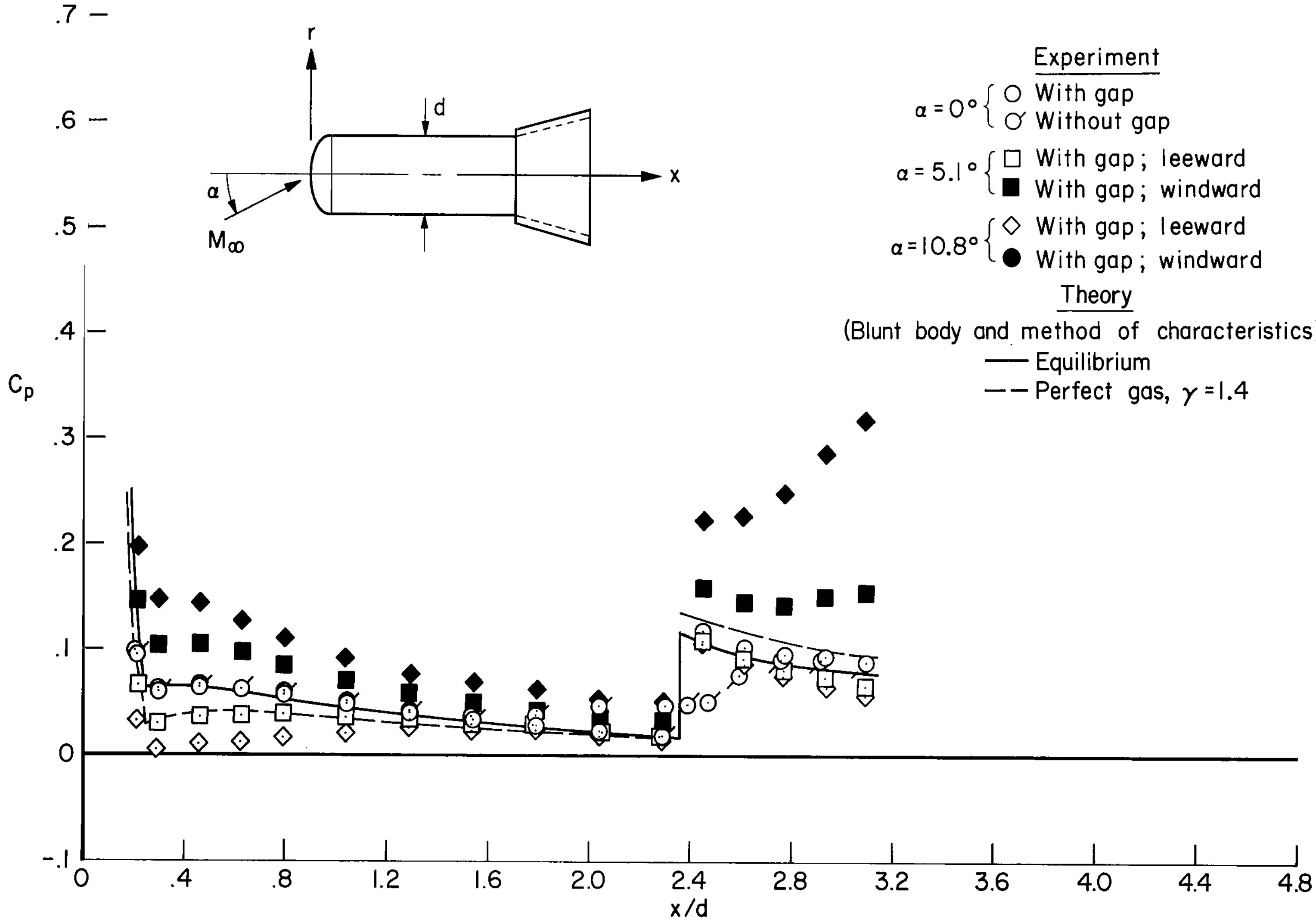

(c) 85-percent CO_2, 15-percent air; $M_\infty = 5.7$

Figure 4.- Concluded.

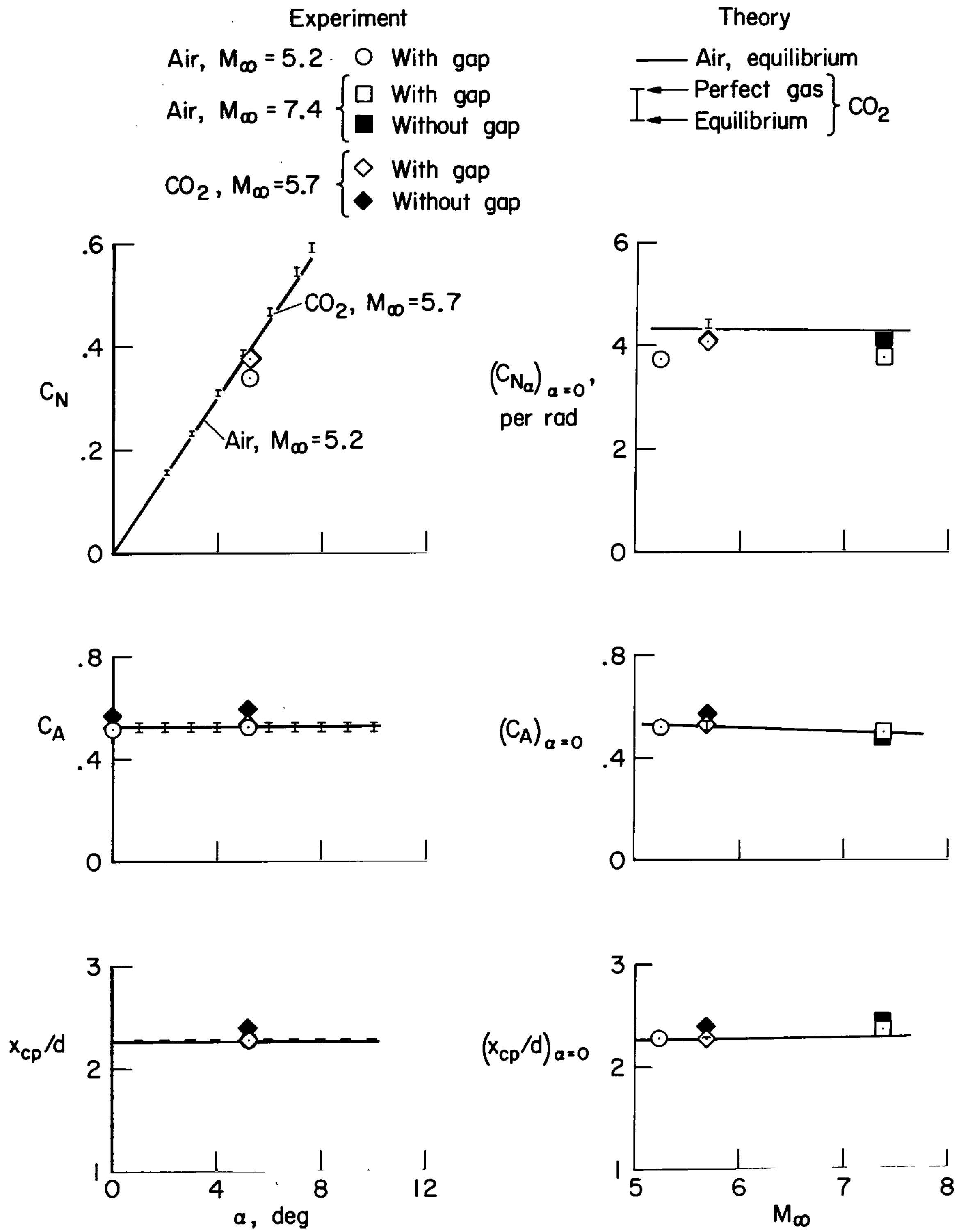

Figure 5.- Comparison of measured and predicted force coefficients for the conical-nosed model.

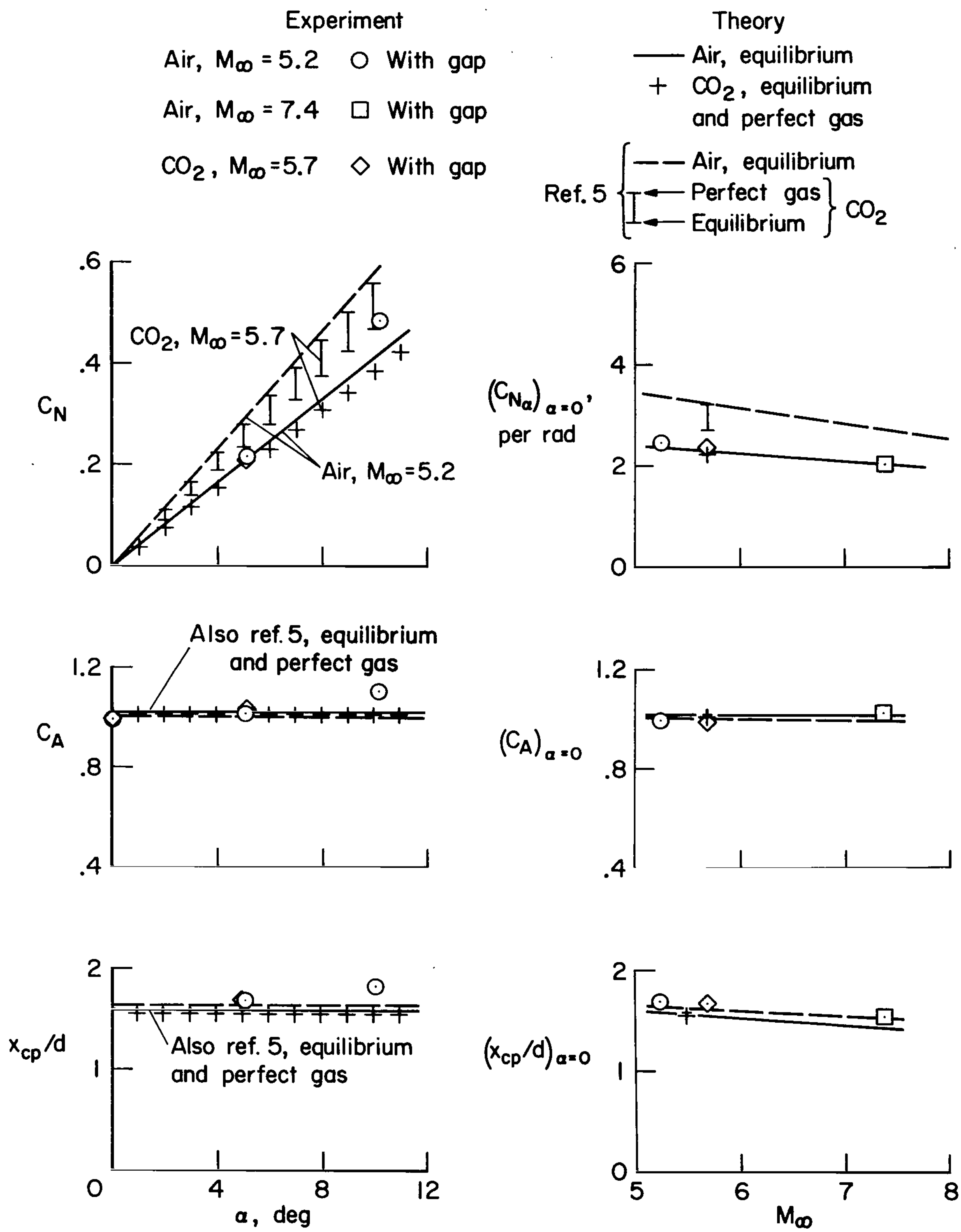

Figure 6.- Comparison of measured and predicted force coefficients for hemispherical-nosed model.

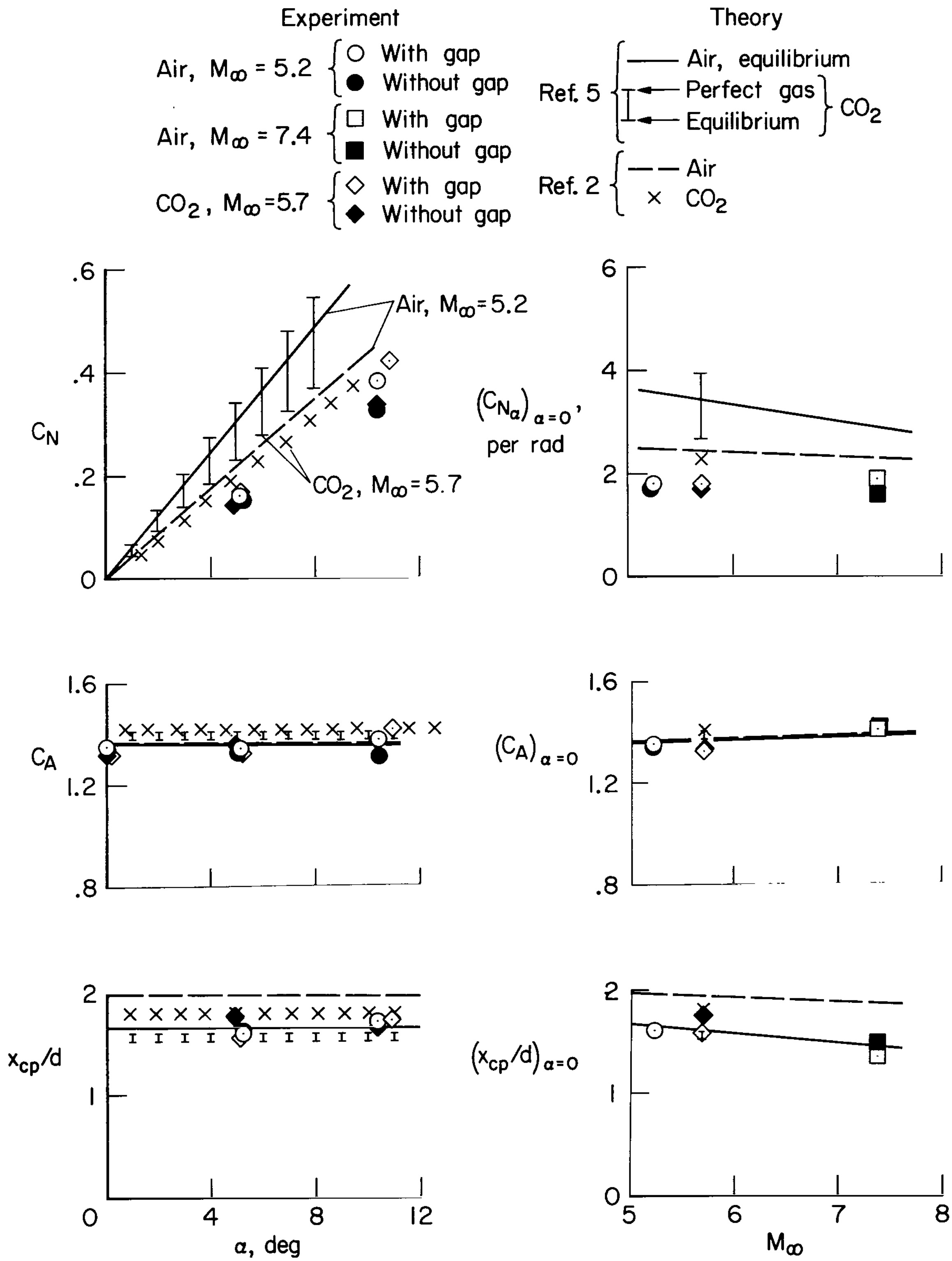

Figure 7.- Comparison of measured and predicted force coefficients for near ellipsoidal-nosed model.

NASA-Langley, 1967 —— 12 A-2678

"The aeronautical and space activities of the United States shall be conducted so as to contribute . . . to the expansion of human knowledge of phenomena in the atmosphere and space. The Administration shall provide for the widest practicable and appropriate dissemination of information concerning its activities and the results thereof."

—NATIONAL AERONAUTICS AND SPACE ACT OF 1958

NASA SCIENTIFIC AND TECHNICAL PUBLICATIONS

TECHNICAL REPORTS: Scientific and technical information considered important, complete, and a lasting contribution to existing knowledge.

TECHNICAL NOTES: Information less broad in scope but nevertheless of importance as a contribution to existing knowledge.

TECHNICAL MEMORANDUMS: Information receiving limited distribution because of preliminary data, security classification, or other reasons.

CONTRACTOR REPORTS: Scientific and technical information generated under a NASA contract or grant and considered an important contribution to existing knowledge.

TECHNICAL TRANSLATIONS: Information published in a foreign language considered to merit NASA distribution in English.

SPECIAL PUBLICATIONS: Information derived from or of value to NASA activities. Publications include conference proceedings, monographs, data compilations, handbooks, sourcebooks, and special bibliographies.

TECHNOLOGY UTILIZATION PUBLICATIONS: Information on technology used by NASA that may be of particular interest in commercial and other non-aerospace applications. Publications include Tech Briefs, Technology Utilization Reports and Notes, and Technology Surveys.

Details on the availability of these publications may be obtained from:

SCIENTIFIC AND TECHNICAL INFORMATION DIVISION

NATIONAL AERONAUTICS AND SPACE ADMINISTRATION

Washington, D.C. 20546